The Effect of Protein Dielectric Coefficient on the Ionic Selectivity of a Calcium Channel

Supplementary material

Dezső Boda[1,2*], Mónika Valiskó[2], Bob Eisenberg[1], Wolfgang Nonner[3], Douglas Henderson[4], Dirk Gillespie[1]
[1]*Department of Molecular Biophysics and Physiology, Rush University Medical Center, Chicago, IL 60612*
[2]*Department of Physical Chemistry, University of Veszprém, P.O. Box 158, H-8201 Veszprém, Hungary*
[3]*Department of Physiology and Biophysics, University of Miami School of Medicine, Miami, FL 33101 and*
[4]*Department of Chemistry and Biochemistry, Brigham Young University, Provo, UT 84602*
(Dated: May 16, 2006)

Parametrization of the surface

Two-dimensional surfaces such as those used in this work can be parameterized using two variables t and ϕ. The transforms that converts these variables into Cartesian coordinates are

$$x = X(t,\phi) \qquad y = Y(t,\phi) \qquad z = Z(t,\phi) \tag{1}$$

and the corresponding area element is

$$A(t,\phi) = \sqrt{\left(\frac{\partial(X,Y)}{\partial(t,\phi)}\right)^2 + \left(\frac{\partial(Y,Z)}{\partial(t,\phi)}\right)^2 + \left(\frac{\partial(Z,X)}{\partial(t,\phi)}\right)^2} \tag{2}$$

where

$$\frac{\partial(X,Y)}{\partial(t,\phi)} = \begin{vmatrix} \frac{\partial X}{\partial t} & \frac{\partial X}{\partial \phi} \\ \frac{\partial Y}{\partial t} & \frac{\partial Y}{\partial \phi} \end{vmatrix} \tag{3}$$

The (outward) unit normal vector is

$$\mathbf{n}(t,\phi) = \frac{\left(\frac{\partial X}{\partial t}, \frac{\partial Y}{\partial t}, \frac{\partial Z}{\partial t}\right) \times \left(\frac{\partial X}{\partial \phi}, \frac{\partial Y}{\partial \phi}, \frac{\partial Z}{\partial \phi}\right)}{\left|\left(\frac{\partial X}{\partial t}, \frac{\partial Y}{\partial t}, \frac{\partial Z}{\partial t}\right) \times \left(\frac{\partial X}{\partial \phi}, \frac{\partial Y}{\partial \phi}, \frac{\partial Z}{\partial \phi}\right)\right|} \tag{4}$$

If a portion of the surface is defined by the X, Y, Z functions over intervals $[t_1,t_2]$ and $[\phi_1,\phi_2]$, then these intervals are divided into N_t and N_ϕ subintervals $\{\Delta t_i\}$ and $\{\Delta\phi_j\}$. The discretization of the $[t_1,t_2]$ and $[\phi_1,\phi_2]$ intervals does not have to be uniform; we can define smaller tiles in regions where we know that electric fields and/or the concentration of source charges is higher. For example, in the selectivity filter we use a fine grid with tile width about 1 Å, while far from the filter, at the outer surface of the protein we use tiles as large as 5 Å.

The center of area of tile (i,j) is defined as

$$\bar{t}_i = \frac{\int\int_{(i,j)} tA(t,\phi)dtd\phi}{\int\int_{(i,j)} A(t,\phi)dtd\phi} \tag{5}$$

and similarly for $\bar{\phi}_j$. The integrals are taken over the given tile. The integral of a vector field $\mathbf{V}$ analogous to that in the matrix then can be given as

$$\int \mathbf{V}(\mathbf{s}-\mathbf{s}^*)\cdot\mathbf{n}(\mathbf{s})\,d\mathbf{s}^* = \sum_{i=1}^{N_t}\sum_{j=1}^{N_\phi} \mathbf{V}(t,\phi,\bar{t}_i^*,\bar{\phi}_j^*)\cdot\mathbf{n}(t,\phi)A(\bar{t}_i^*,\bar{\phi}_j^*)\Delta t_i^*\Delta\phi_j^* \tag{6}$$

* Author of correspondence, E-mail: dezso_boda@rush.edu

where vector $\mathbf{s}$ is parametrized by the parameters t and ϕ, while $\bar{t}_i^*$ and $\bar{\phi}_j^*$ are the centers of the tiles over which the double sum runs.

The above description does not specify what is the surface over which the integral is taken. It can be a tile of the whole protein; in that case the above discretization is really a subdiscretization. The meaning of the variables can be different in various portions of the surface depending on its symmetry. For example, the model shown in Fig. 1 has a rotational symmetry: the surface of the protein is obtained as a surface of revolution about the z-axis. The formulas then can be simplified as

$$x = R(t)\cos\phi \qquad y = R(t)\sin\phi \qquad z = z(t) \tag{7}$$

$$A(t,\phi) = R(t)\sqrt{(z'(t))^2 + (R'(t))^2} \tag{8}$$

and

$$\mathbf{n}(t,\phi) = \frac{(z'(t)\cos\phi, z'(t)\sin\phi, -R'(t))}{\sqrt{(z'(t))^2 + (R'(t))^2}} \tag{9}$$

The primes in the last two equations denote differentiation with respect to t. In the case of the protein shown in Fig. 1, variable ϕ is the rotational angle, while variable t is defined differently in the various regions of the surface: (1) in the case of the cylinders (such as that confining the filter) $z = t$ and $R = const.$, (2) on the flat walls $z = const.$ and $R = t$, while (3) at the rounded corners t can be defined as an angle.

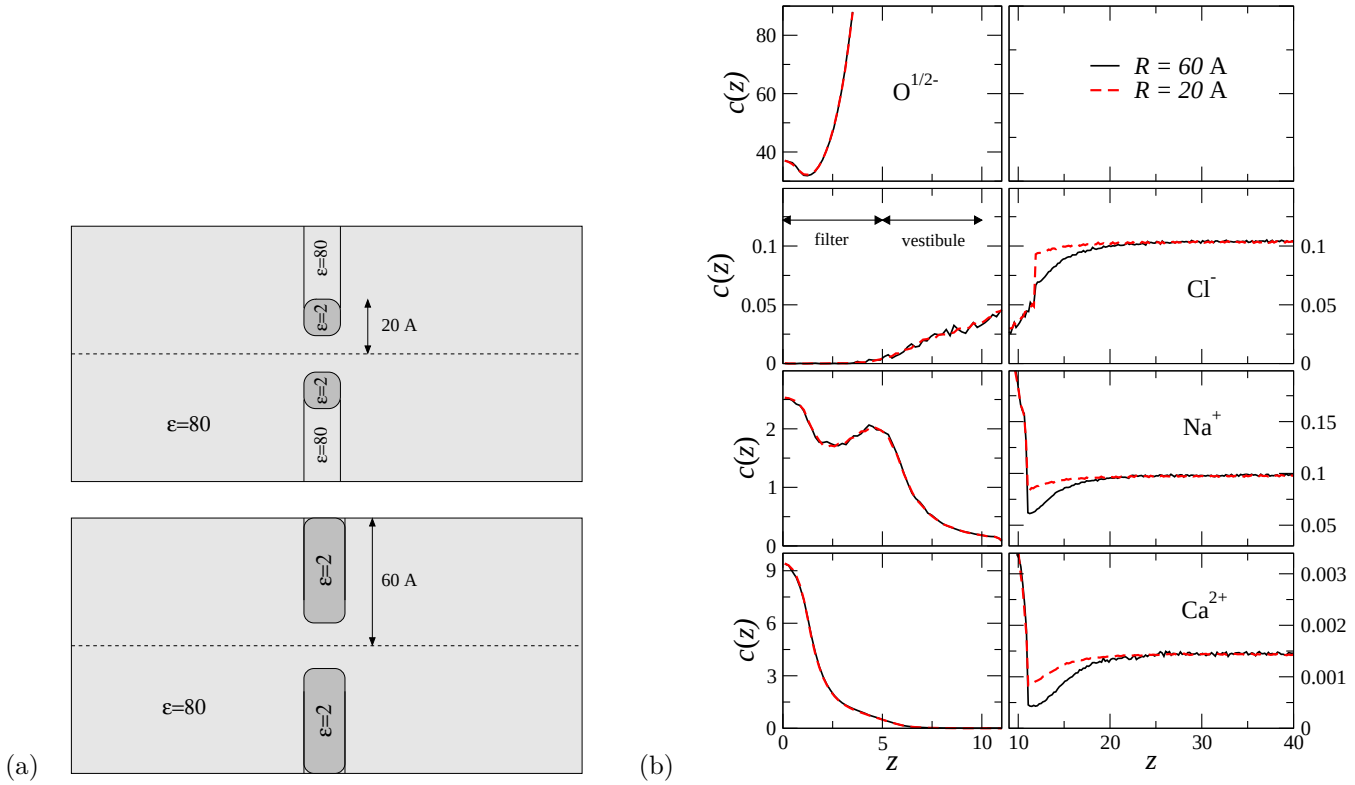

Supplementary Figure 1 The dielectric constant of the membrane was 80 in our simulations to save computer time by avoiding the appearance of induced charge on the membrane-solution boundaries. Because the dielectric constant of the membrane is lower than that of the solution, we performed an additional simulation for a given state point with the protein extending up to the outer wall of the simulation cell. This geometry corresponds to a situation when the dielectric constant of the membrane is the same as that of the protein. The figure shows the density profiles obtained for these two geometries. The only significant difference between the two situations arise just outside the channel at the walls of the membrane. In the case of $R = 60$ Å when the low dielectric domain is extended up to the cell boundary, the density profiles decline more approaching the membrane due to the additional repulsive charges induced on the now larger dielectric boundaries. Nonetheless, this region is in between the filter and the bath, the two regions are interest, whose interaction and exchange of ions determines selectivity. The ionic profiles in these regimes are unchanged. Therefore, the assumption of assigning 80 dielectric constant to the membrane does not alter our conclusions regarding selectivity.

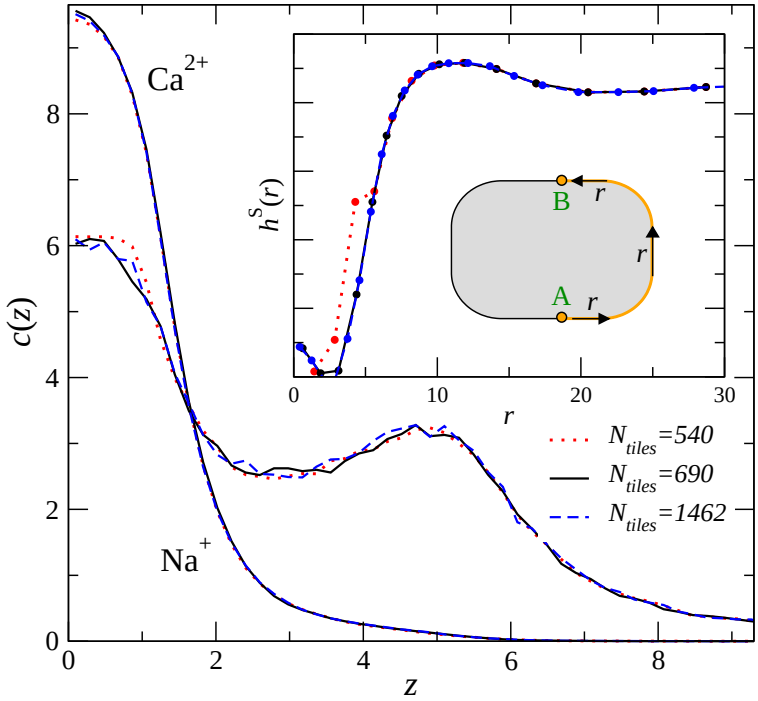

Supplementary Figure 2 The longitudinal density profiles of Ca^{2+} and Na^{+} ions for varying resolution of the grid. The number of tiles 540, 690, and 1462 correspond to Δx = 1.43, 1.25, and 0.84 Å, respectively, where Δx is the width of the tiles in the filter. The simulations were performed for $\epsilon = 10$ and $[CaCl_2]$=8.6×10^{-5} M. The inset shows the distribution of the induced charge density along a path starting in the middle of the filter (point A) and ending in the middle of the outer bounding cylinder (point B). The surface charge is averaged over the angle of revolution and the two symmetric sides of the protein. The induced charge profile is the same for the two better resolutions, while it shows some deviation for $N_{tiles} = 540$. The influence of the errors in $h(r)$ on the ionic density profiles is negligible within the statistical noise and even the smallest number of tiles (540) gives accurate profiles.

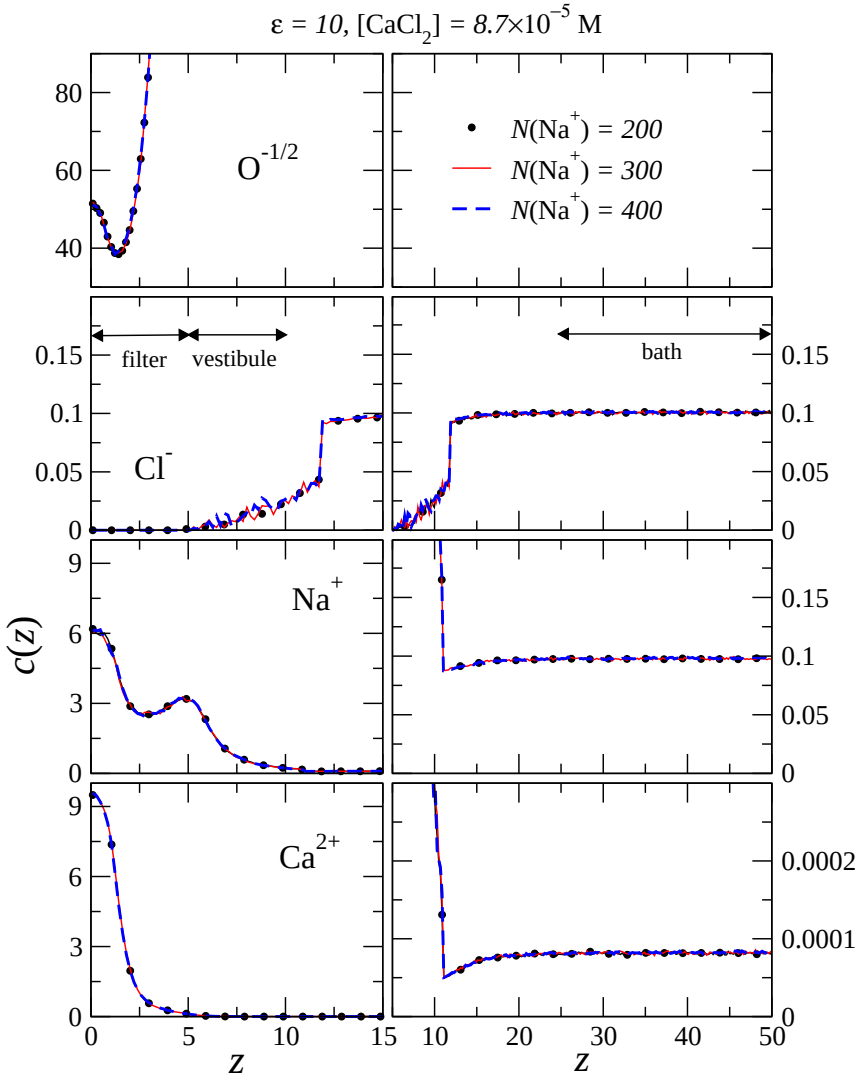

Supplementary Figure 3 The density profiles of the various ions for different system sizes (number of sodium ions).

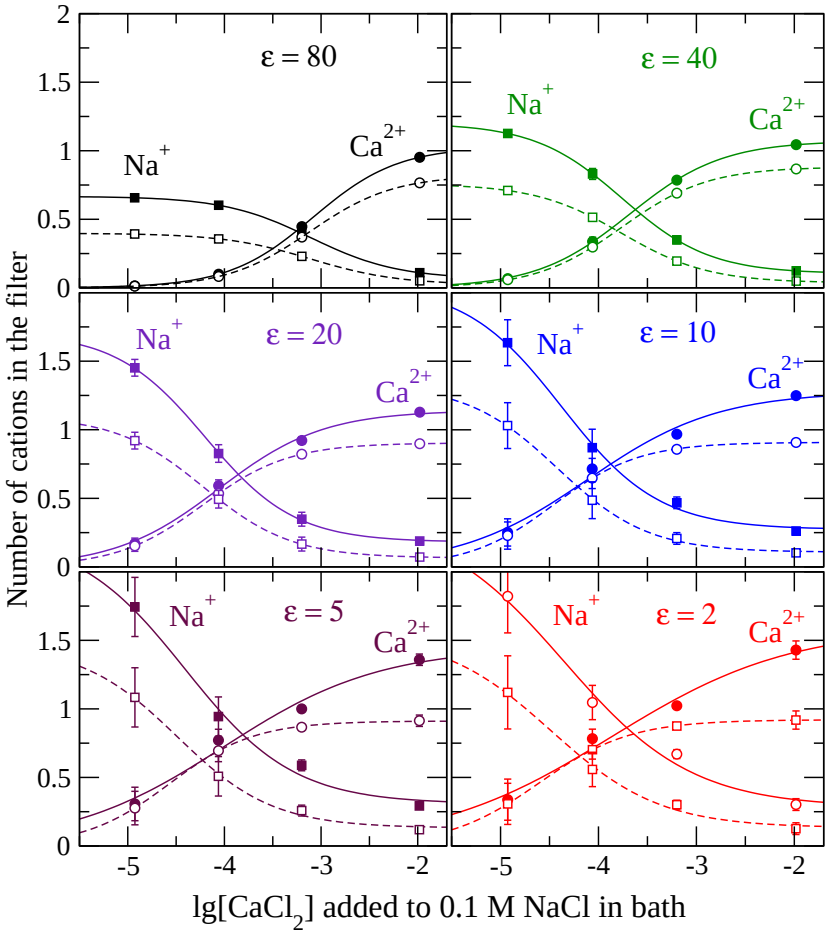

Supplementary Figure 4 The average numbers of Na^+ and Ca^{2+} ions with centers in specified regions of the cylindrical pore ($|z| \leq \Delta H/2$) versus the logarithm of $CaCl_2$ concentration in the bath; the bath concentration of NaCl is maintained at 0.1 M. Various insets of the figure refer to various dielectric coefficients of the protein. The symbols with error bars are simulation results; the curves are fits to aid the eye; the fit included a point obtained in the absence of $CaCl_2$ (not shown). Solid and dashed lines refer to integration over the whole pore ($\Delta H = 10$ Å) and the central pore ($\Delta H = 4.2$ Å), respectively. Circles and squares denote Ca^{2+} and Na^+, respectively.